



Experiments on cold-formed ferritic stainless steel slender sections



M. Bock*, I. Arrayago, E. Real

Department of Construction Engineering, Universitat Politècnica de Catalunya, UPC, C/Jordi Girona 1-3, 08034 Barcelona, Spain

ARTICLE INFO

Article history:

Received 14 October 2014

Accepted 16 February 2015

Available online 13 March 2015

Keywords:

Effective width

Element interaction

Experiments

Ferritic stainless steel

Slenderness limits

Local buckling

ABSTRACT

The usage of stainless steel in construction has been increasing owing to its corrosion resistance, aesthetic appearance and favourable mechanical properties. The most common stainless steel grades used for structural applications are austenitic steels. The main drawback of these grades relies on their nickel content (around 8–10%), resulting in a relatively high initial material cost. Other stainless steel grades with lower nickel content such as the ferritic steels offer the benefits of stainless steels in terms of functional qualities and design but within a limited cost frame. Hence, ferritic stainless steels may be a viable alternative for structural applications. Given the fact that little experimental information on ferritic stainless steels is currently available, the purpose of this investigation is to report a series of material and cross-section tests on ferritic grade EN 1.4003 (similar to 3Cr12) stainless steel square and rectangular hollow sections to enable a better understanding of their material response and structural performance. Four different cross-section geometries have been tested under pure compression and in-plane bending. Measurements of geometric imperfections and material properties are also presented. The obtained test results are used to assess the adequacy of the slenderness limits and effective width formula given in EN 1993-1-4 to ferritic stainless steels, those proposed by Gardner and Theofanous and Zhou et al. design approach.

© 2015 Elsevier Ltd. All rights reserved.

1. Introduction

The chromium present within the internal crystalline structure of stainless steels forms a self-healing passivation layer of chromium oxide (Cr_2O_3) when exposed to oxygen preventing surface corrosion. Other alloying elements are added to meet specific needs in terms of strength, corrosion resistance and ease of fabrication. Depending on their chemical composition, stainless steels can be classified into main five categories: ferritic, austenitic, martensitic, duplex and precipitation hardening. The most commonly used materials in construction are the austenitic grades which have reasonable mechanical strength with 0.2% proof stress of 210–240 N/mm² and display high ductility with ultimate strains ϵ_u laying between 50 and 60%. These positive features, however, may be inhibited by the high initial material cost and considerable price fluctuations associated with the amount of nickel involved in austenitic stainless steels (8–11%). Ferritic stainless steels, on the other hand, contain little nickel leaving chromium as the main alloying element (min. 10.5%); hence, they are price stable and cheaper alloys. In comparison with the austenitic grades, the initial material cost of ferritic stainless steels is about three times lower which makes them an attractive alternative for structural applications. Despite their low nickel content, which may reduce ductility and increase risk of pitting corrosion, ferritic stainless steels offer a good combination of mechanical and

corrosion-resistance properties with higher 0.2% proof stress of 250–330 N/mm² in the annealed condition and they are easier to work and machine in comparison with the austenitics. Moreover, by increasing the chromium content (10.5–30%) and including establishing alloying elements such as molybdenum and niobium, similar corrosion resistance to some austenitics grades can be achieved without compromising the initial material cost.

The viability of ferritic stainless steels for structural applications has been recently investigated within the framework of a RFCS European project [2] where the applicability of various aspects of the European design guidance for stainless steels, EN 1993-1-4 [1], to this material was examined. The specifications for cross-section design given in EN 1993-1-4 [1], have been assessed for application to ferritic stainless steel on the basis of experimental data [3–5] and generated numerical models within the context of that European project [6]. However, a fully experimental validation is yet required especially for cross-sections comprising slender elements. Hence, the purpose of this paper is to describe a comprehensive laboratory testing program on grade 1.4003 stainless steel slender tubular sections featuring square and rectangular hollow sections (SHS and RHS, respectively) conducted at the Universitat Politècnica de Catalunya. A total of 8 stub column tests and 9 beam tests, including 3-point bending and 4-point bending configurations were carried out. The mechanical material properties were determined at Acerinox Europa S.A.U where 16 tensile coupon tests, including both flat and corner specimens, were performed. The obtained test results have been used to assess the applicability of the slenderness limits and the accuracy of the effective width equations

* Corresponding author. Tel.: +34 934054156; fax: +34 934054135.
E-mail address: marina.bock@upc.edu (M. Bock).

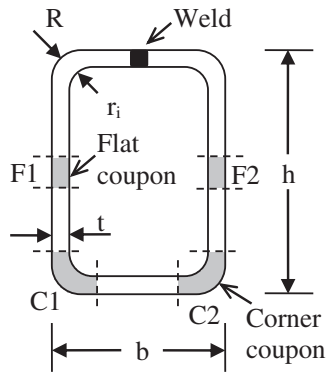


Fig. 1. Definition of symbols and location of coupon in cross-section.

for slender elements given in EN 1993-1-4 [1]. The revised slenderness limits and effective width formula proposed by Gardner and Theofanous [7] as well as the design approach derived by Zhou et al. [8] have also been considered herein. Relevant conclusions regarding various appraisals are presented and design recommendations are proposed.

2. Experimental investigation

2.1. Introduction

An experimental investigation including 8 stub column tests and 9 beam tests was performed on ferritic stainless steel SHS and RHS in the Laboratori de Tecnologia d'Estructures Luis Agulló, in the Department of Construction Engineering at Universitat Politècnica de Catalunya. Four section sizes were examined ($h \times b \times t$): SHS $60 \times 60 \times 2$, RHS $70 \times 50 \times 2$, RHS $80 \times 40 \times 2$ and RHS $100 \times 40 \times 2$, see Fig. 1. The investigated sections provided height to width ratios of 1, 1.4, 2 and 2.5. The specimens were cold-rolled from annealed flat strips of 1.4003 stainless steel and were delivered by the manufacturer in appropriate lengths to perform material and structural tests. The chemical composition and the tensile properties of the coil material used to form the various specimens are given in Table 1 and Table 2, respectively, as provided by the steelmaker in the mill certificates.

2.2. Material tests

A series of tensile coupon tests were conducted at Acerinox Europa S.A.U to determine the basic stress–strain response of the ferritic stainless steel specimens. All the tested coupons were extracted from the batch of the specimens selected for the tests. Two tensile flat coupons were taken from two faces of the SHS and RHS specimens in the longitudinal direction, resulting in a total of 8 tensile coupon tests. All tensile flat coupons were machined into parallel necked specimens with a standard gauge length of $5.65 \sqrt{A_c}$, where A_c is the cross-sectional area of the coupon, and width of 15 mm. Additional corner coupons were extracted from the curved portions of each of the cross-sections extended two times the thickness through the flat region in

Table 2
Mechanical properties from mill certificates.

| Section | $\sigma_{0.2}$ (MPa) | $\sigma_{1.0}$ (MPa) | σ_u (MPa) | ϵ_f |
|----------------------------------|----------------------|----------------------|------------------|--------------|
| SHS $60 \times 60 \times 2$ -T1 | 355 | 379 | 491 | 0.41 |
| SHS $60 \times 60 \times 2$ -T2 | 342 | 363 | 479 | 0.40 |
| RHS $70 \times 50 \times 2$ -T1 | 349 | 371 | 496 | 0.38 |
| RHS $70 \times 50 \times 2$ -T2 | 350 | 368 | 484 | 0.40 |
| RHS $80 \times 40 \times 2$ -T1 | 353 | 377 | 501 | 0.38 |
| RHS $80 \times 40 \times 2$ -T2 | 351 | 372 | 496 | 0.37 |
| RHS $100 \times 40 \times 2$ -T1 | 373 | 408 | 529 | 0.23 |
| RHS $100 \times 40 \times 2$ -T2 | 350 | 379 | 498 | 0.24 |

order to quantify the corner strength enhancements induced by the cold-forming process [9,10]. A total of 16 material tests were performed.

Having extracted both flat and corner coupon tests, a longitudinal curving of all coupon specimens was observed. This was due to the release of the through-thickness bending residual stresses induced during the manufacturing process and present in the final cross-section. All the coupons almost returned to their flat state during gripping in the testing machine's jaws [11,12]. Hence, the obtained stress–strain responses inherently include the effect of longitudinal through-thickness bending residual stresses. Membrane residual stresses were not explicitly measured since previous studies [13,14] concluded that their effect is relatively small compared to bending residual stresses.

The coupons were placed in a hydraulic machine (see Fig. 2(a)) and were tested according to [15]. The test were conducted at uniform strain rate of 0.00025 s^{-1} up to the 0.2% proof stress and then increased up to 0.008 s^{-1} until fracture. A data acquisition system was employed to record load and displacement at regular intervals while testing by using a data logger piece of software. Typical tensile coupon fractures are presented in Fig. 2(b) and (c) for the flat and the corner coupons, respectively.

The material properties obtained from the coupon tests are summarized in Table 3 where the coupons have been labelled beginning with the section geometry e.g. SHS $60 \times 60 \times 2$, followed by the coupon type, F for tensile flat, C for tensile corner, and finally the section face number (1, 2), as given in Fig. 1. The material parameters reported in Table 3 are the Young's modulus E , the dynamic 0.01%, 0.05% and 0.2% proof stresses $\sigma_{0.01}$, $\sigma_{0.05}$ and $\sigma_{0.2}$ respectively, and the maximum achieved ultimate tensile stress σ_u with its corresponding ultimate strain ϵ_u . These material property values can be used to replicate the whole stress–strain curve on the basis of the compound Ramberg–Osgood material models available in the literature [16–19]. The weighted average material properties based on face width and corner properties extended two times the thickness through the flat region of each section are given in Table 4. Typical stress–strain response of tensile flat and tensile corner ferritic stainless steel material are depicted in Fig. 3.

2.3. Stub column tests

Two repeated concentric stub column tests were performed on four ferritic stainless steel slender cross-sections: SHS $60 \times 60 \times 2$, RHS $70 \times 50 \times 2$, RHS $80 \times 40 \times 2$ and RHS $100 \times 40 \times 2$. All the specimens were selected to be short enough to avoid global flexural buckling but

Table 1
Chemical composition of grade EN 1.4003 stainless steel from mill certificates.

| Section | C % | Si % | Mn % | P % | S % | Cr % | Ni % | N % | CO % |
|------------------------------|-------|-------|-------|-------|-------|--------|-------|-------|-------|
| SHS $60 \times 60 \times 2$ | 0.012 | 0.250 | 1.440 | 0.029 | 0.002 | 11.300 | 0.400 | 0.016 | 0.010 |
| RHS $70 \times 50 \times 2$ | 0.012 | 0.290 | 1.440 | 0.030 | 0.001 | 11.200 | 0.400 | 0.009 | 0.010 |
| RHS $80 \times 40 \times 2$ | 0.012 | 0.280 | 1.400 | 0.030 | 0.001 | 11.400 | 0.400 | 0.010 | 0.010 |
| RHS $100 \times 40 \times 2$ | 0.015 | 0.370 | 1.480 | 0.027 | 0.002 | 11.200 | 0.400 | 0.009 | 0.010 |

Download English Version:

<https://daneshyari.com/en/article/284471>

Download Persian Version:

<https://daneshyari.com/article/284471>

[Daneshyari.com](https://daneshyari.com)